Arch. Metall. Mater. **70** (2025), 1, 509-514

DOI: https://doi.org/10.24425/amm.2025.152571

HAODONG LIU[1*], LIUQING HUANG[1], DONGSHENG WANG[2], CHANGJUN CHEN[3],
AIYONG CUI[1], SHIKANG DONG[1], ZHIWEI DUAN[1]

PREPARATION PROCESS OF WC WEAR-RESISTANT COATING ON TITANIUM ALLOYS USING ELECTRO-SPARK DEPOSITION

Due to their excellent corrosion resistance and high specific strength, Ti alloys are widely used in shipboard aircraft structures. However, their low wear resistance limits further applications. In this study, wear-resistant tungsten carbide (WC) coatings were applied to TC4 alloy using electro-spark deposition (ESD), and the processing parameters were optimized through orthogonal testing. The effects of ESD processing parameters on the surface morphology of the wear-resistant WC coating were also investigated. The results showed that output voltage, deposition frequency, and electrode speed significantly influenced coating morphology. A relatively flat and uniform coating on the titanium alloy surface was achieved with WC coatings prepared under an output voltage of 120 V, deposition frequency of 120 Hz, and electrode speed of 350 r.

Keywords: Electro-spark deposition (ESD); Ti alloys; WC; Wear-resistant coating; Surface morphology

1. Introduction

With the rapid development of naval aviation, flight training tasks are increasing, and mission execution conditions are becoming more demanding. Current shipboard aircraft need to operate stably for extended periods under high-speed, high-load, and high-temperature conditions, placing greater demands on the wear resistance of mechanical equipment. Ti alloys are gradually replacing Al alloys in shipboard aircraft due to their low density, high specific strength, and excellent corrosion resistance [1-3]. As the number of shipboard aircraft in China increases and the operational environment becomes more complex, the demand for Ti alloys also rises. Ti alloys are not only used in aircraft structural components but are also widely utilized in engine parts, landing gear, fasteners, and other critical components. However, Ti alloys are limited by low hardness and wear resistance, making them prone to adhesive wear, which restricts their use in high-stress, high-friction environments. Therefore, improving the hardness and wear resistance of Ti alloys has become a key focus of research and application [4].

Electro-spark deposition (ESD) is a process in which electrode material is melt-infiltrated into the surface layer of a workpiece via spark discharge to form an alloyed surface deposition layer. This technique has been widely used for surface strengthening of Ti alloy components in aerospace engines [5]. ESD has a broad range of applications, not only in the aerospace industry but also in other high-end manufacturing fields such as the nuclear industry and electronic equipment. Its process characteristics allow for the formation of uniform, compact coatings on complex shapes and hard-to-process materials, significantly improving the service life and reliability of parts [6]. By continuously optimizing ESD processing parameters and developing new electrode materials, its effectiveness and range of applications can be further enhanced [7,8]. The published literature on the application of wear-resistant coatings has focused on metallic ceramic coatings such as TiC and TiN, but the coatings tend to be too thin and too brittle, and has too many defects, making them unsuitable for the surface strengthening of the titanium alloy. W element in WC has the function of strengthening matrix, whereas C element has the effect of enhancing alloy hardness and strength, and has good cost performance. Therefore it is suitable for reinforcement on titanium alloy surfaces. Zhong et al. [9] prepared the Zr-based alloy coating on the surface of ZL101 aluminum alloy using ESD technology and applied the control variables to optimize the process parameters. Zhao et al. [10] prepared Ni201 modified coating on the surface of Q235 steel

---

[1] NAVAL AVIATION UNIVERSITY QINGDAO BRANCH, QINGDAO, 266041, P.R. CHINA
[2] WUXI JINYAN LASER GAS TURBINE PARTS CO., LTD, WUXI, 214429, P.R. CHINA
[3] SCHOOL OF MECHANICAL AND ELECTRIC ENGINEERING, SOOCHOW UNIVERSITY, SUZHOU, 215021, P.R. CHINA

[*] Corresponding author: mdlhd@sina.com

by ESD and analyzed the influence of arc ratio on the modified coating quality at different values. Wang et al. [11] designed and conducted the ESD orthogonal test under the line contact of the cylindrical electrode and the matrix, the influence of the electrode diameter, electrode thickness, and electrod speed on the deposition efficiency and the coating surface roughness were analyzed, and the cylindrical electrode process parameters was optimized.

2. Materials and method

A TC4 alloy sheet measuring 100 mm × 100 mm × 1 mm was used for the tests. All tests were conducted on this sheet to ensure comparability and reproducibility of the results. TC4 alloy (Ti-6Al-4V) is one of the most widely used Ti alloys, with its main chemical compositions and mechanical strength presented in TABLES 1 and 2, respectively [12]. TC4 alloy offers high strength, low density, good corrosion resistance, and excellent high-temperature performance, making it particularly suitable for manufacturing aircraft engine components, fuselage structural components, and marine propulsion systems that operate under high stress and in corrosive environments [13-14].

With its extremely high hardness and wear resistance, WC has been widely used in cutting tools, wear-resistant parts, and surface coatings [15]. It is typically employed to enhance the wear resistance of metals. Additionally, WC exhibits a high melting point, along with excellent thermal and electrical conductivities.

The test was conducted using the TLB-V multi-functional metal surface strengthening cold patching machine (Beijing Tianchengyu New Material Technology Co.), with its performance indicators shown in TABLE 3. Ar (purity = 99.99%) was used as a protective gas for coaxial protection, with a fixed gas flow rate of 7 L/min.

The processing parameters of ESD were optimized using an orthogonal test. Three processing parameters – output voltage, deposition frequency, and electrode speed – were selected as the main factors with significant effects on the experimental results.

TABLE 1

Chemical composition of TC4 alloy

Element	Ti	Al	V	Fe	O	C	N	H
Measured value (%)	Remaining	5.5-6.75	3.5-4.5	≤0.30	≤0.20	≤0.08	≤0.05	≤0.015

TABLE 2

Mechanical strength of TC4 alloy

Index	Tensile strength	Yield strength	Elongation	Section shrinkage	Hardness	Fatigue strength
Value	≥895 MPa	≥825 MPa	≥ 10%	≥25%	32 HRC	510 MPa

TABLE 3

TLB-V metal surface strengthening cold patching machine technical parameters

Output frequency /W	Output voltage /V	Discharge frequency /Hz	Welding torch rotation speed /r/min
3000	0-180	30-800	300-800

TABLE 4

Orthogonal testing scheme

Sample No.	Output Voltage/V	Deposition Frequency/Hz	Electrode Speed/r·min^{-1}
1	100	60	350
2	100	90	400
3	100	120	450
4	100	150	500
5	110	60	400
6	110	90	350
7	110	120	500
8	110	150	450
9	120	60	450
10	120	90	500
11	120	120	350
12	120	150	400
13	130	60	500
14	130	90	450
15	130	120	400
16	130	150	350

Four different levels were set for each main factor according to the pre-test results, with each level representing a different possible state of the factor in the experiment. The orthogonal table (TABLE 4) was chosen for the experimental design based on the number of factors and levels. This three-factor, four-level orthogonal test examined three factors, each with four level combinations in the experimental design. The levels of each factor were assigned to the columns of the orthogonal table to form the experimental protocol. After deposition, metallographic samples were prepared, and the coating surface was observed using a super depth-of-field microscope to analyze the macroscopic morphology and defects of the coatings. The roughness features in the images were measured, labeled, and statistically analyzed. Four 2-cm coating samples were prepared for each test group to evaluate the deposition quality of the coating, as shown in Fig. 1.

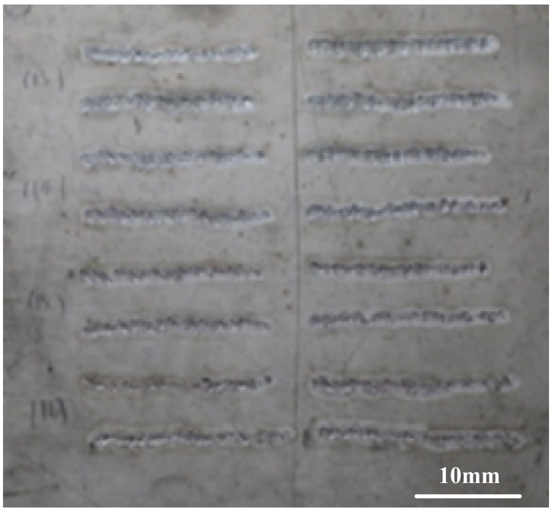

Fig. 1. Wear-resistant WC coatings prepared by surface deposition on Ti alloys

3. Results and discussion

3.1. Effect of processing parameters on the surface morphology of the coating

A super depth-of-field microscope was used to scan the surface and obtain load curves and a diagram of volume parameters in this test. *Sk*, *Spk*, and *Svk* were extracted from the load curve (TABLE 5), while *Vmp*, *Vmc*, and *Vvv* were extracted from the diagram of volume parameters. By observing the shape of the load curve, the distribution characteristics of surface roughness can be assessed. A flatter load curve indicates low surface roughness, while a steeper load curve indicates high surface roughness. Combined with *Sk* and the volume parameters, surface roughness is evaluated comprehensively to assess surface quality and performance.

Sk parameters are a common set of parameters used in surface morphology analysis, which can be read and analyzed from the load curve. *Sk* refers to the height of the core of the surface profile, reflecting the height distribution in the middle region of the surface: high *Sk* means that the middle region of the surface profile is flatter, with less roughness in the core region; while a lower *Sk* indicates a more variable height in the core area and a rougher surface. Peak height (*Spk*) refers to the peak height of the surface profile, which represents the height of the highest point on the surface: high *Spk* means that there are more protrusions and peaks on the surface, which may increase friction and wear, while low *Spk* means that the surface is flatter and has fewer protrusions. Valley depth (*Svk*) refers to the valley depth of the surface profile, which represents the depth of the lowest point on the surface: high *Svk* means that there is a deeper valley depth on the surface, which may become stress concentration

TABLE 5

Surface roughness of different samples

	***Spk*/µm**	***Sk*/µm**	***Svk*/µm**	***Vmp*/µm^3**	***Vmc*/µm^3**	***Vvv*/µm^3**
1	7.916	10.168	5.581	1.035	3.893	1.248
2	9.401	41.964	9.455	2.164	12.262	2.538
3	16.983	29.371	27.924	2.515	10.197	4.283
4	13.749	55.840	22.143	2.198	21.498	4.304
5	19.932	35.624	10.766	4.369	11.701	3.432
6	10.388	28.378	14.678	3.285	9.772	3.789
7	6.631	18.090	29.969	0.394	7.380	3.257
8	14.923	27.849	12.708	2.306	11.858	3.525
9	11.829	31.347	16.124	1.831	10.845	2.429
10	18.097	19.445	8.281	1.419	7.288	0.763
11	20.610	49.757	43.641	1.085	19.57	6.780
12	21.472	32.110	12.492	4.025	11.633	3.928
13	17.100	33.304	10.910	2.370	13.681	4.322
14	13.243	17.049	7.510	2.745	6.658	3.369
15	13.044	26.877	23.111	2.533	10.929	3.494
16	20.494	46.974	11.722	3.734	16.502	3.027
Mean value	14.738	31.509	16.333	2.376	11.604	3.406
Maximum value	21.472	55.840	43.641	43.641	21.498	6.780
Minimum value	6.631	10.168	5.581	0.394	3.893	0.763

sites and wear sites, while low *Svk* means that the surface is flat and the valley depth is shallow.

The diagram of volume parameters usually consists of three regions: peak volume (*Vmp*), core volume (*Vmc*), and valley volume (*Vvv*), which reflect the volume distribution of the surface profile in different height regions. *Vmp* refers to the volume of the highest area of the surface: a high *Vmp* indicates more protrusions, which may increase friction and wear, while a low *Vmp* suggests a smoother surface with fewer protrusions. *Vmc* refers to the volume of the middle region of the surface: a high *Vmc* indicates a flatter middle region with a larger core volume, while a low *Vmc* suggests a smaller core volume and a rougher surface. *Vvv* refers to the volume of the lowest area of the surface: a high *Vvv* indicates more depressions, which may become stress concentration and wear sites, while a low *Vvv* suggests a smoother surface with fewer depressions.

Regarding output voltage, excessively high output voltage leads to stronger discharge, increasing the amount of molten material and spattering, thereby increasing surface roughness. Conversely, excessively low voltage may result in insufficient discharge energy, causing uneven melting and higher surface roughness. An appropriate voltage ensures that the coating surface is sufficiently melted, forming a compact structure and resulting in a smoother surface [16].

For deposition frequency, excessively high deposition frequency results in more discharge, increasing heat accumulation and potentially increasing surface roughness. Conversely, a low deposition frequency leads to longer discharge intervals, potentially prolonging the coating deposition time and affecting surface roughness. Appropriate deposition frequency can reduce the surface roughness and the deposition defects, thereby improving the deposition quality [9].

As for electrode speed, excessively high speed does not allow enough time for the coating to evenly distribute on the surface of the workpiece, potentially leading to uneven deposition. Conversely, excessively low speed may increase deposition time and complicate human operation, affecting the compactness and surface quality. Appropriate electrode speed can obtain uniform dense deposition coating and better deposition quality.

Therefore, by adjusting output voltage, deposition frequency, and electrode speed, the ESD process can be optimized to improve surface roughness. In this study, a relatively flat and uniform coating on the surface of the titanium alloy was achieved with WC coatings prepared at an output voltage of 120 V, deposition frequency of 120 Hz, and electrode speed of 350 r.

3.2. Effects of processing parameters on the macroscopic morphology of the coating

In macroscopic images captured by a super depth-of-field microscope, different colors represent height information on the sample surface. Pseudo-coloring of the height data visualizes surface features and height variations: blue areas indicate the lowest points or depressions, green areas represent medium height regions, and red areas denote the highest points or protrusions. Color coding facilitates the observation and analysis of surface features, helping to identify inhomogeneities, defects, and other important surface characteristics.

The following analyses focus on the surface morphology of two test groups of samples with low surface roughness.

Fig. 2 shows the macroscopic morphology of Sample 1. The results indicate that *Spk*, *Vmp*, *Svk*, and *Vvv* of Sample 1 were significantly poor, suggesting a good surface homogeneity with the absence of large protrusions or depressions. However, *Sk* and *Vmc* were poor, indicating a small core region and higher surface roughness. The color distribution reveals larger and more uniformly distributed blue and green areas, which represent lower surface roughness and better uniformity of the smooth surface area. This reduces surface irregularity and enhances functionality and service life, which is advantageous for applications requiring a low coefficient of friction or high gloss, such as bearing surface, actuator cylinder, and so on. Nonetheless, distinct dark-colored craters were present, attributed to the unevenness

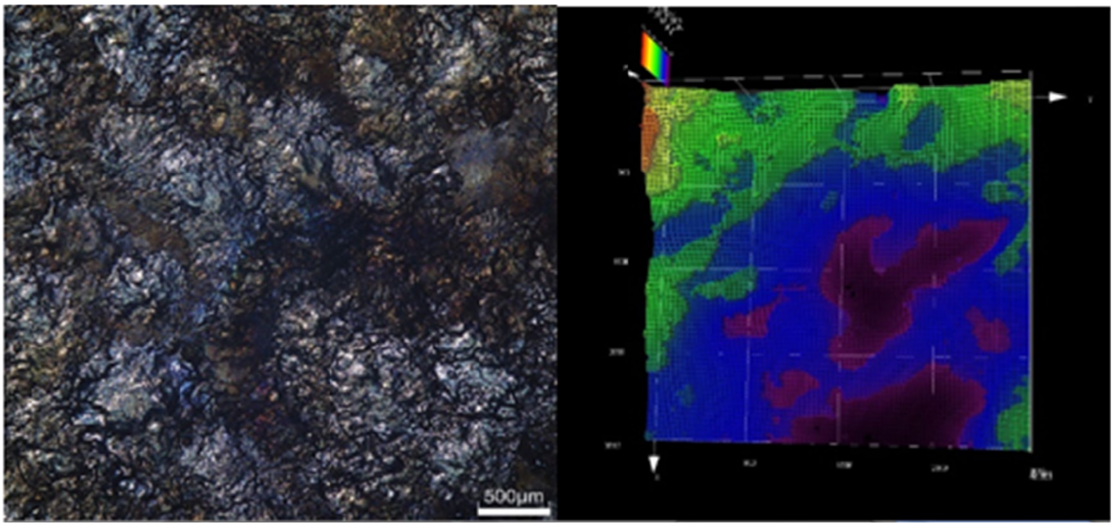

Fig. 2. Surface morphology of Sample 1

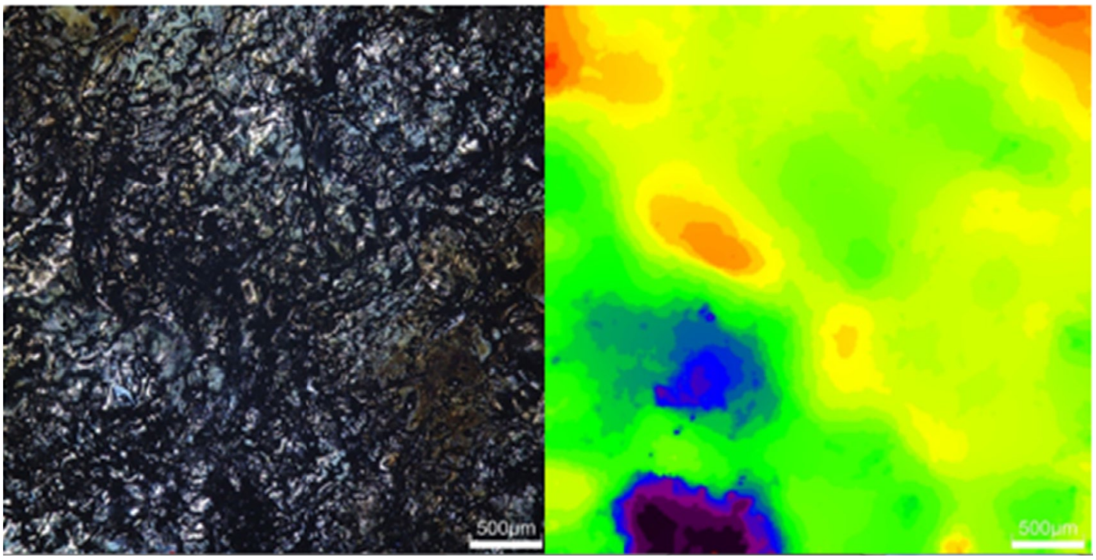

Fig. 3. Surface morphology of Sample 11

of the deposition process. This unevenness, mainly due to the manual operation mode of the ESD deposition gun used in this study, which has the disadvantages of inconsistent movement speed and uneven deposition contact force, leading to the uneven deposition operation process [17-19].

Fig. 3 shows the macroscopic morphology of Sample 11. Data processing revealed both better and worse performance metrics within this group, necessitating separate analysis. The image indicates that, despite surface inhomogeneity, the distribution of different colored areas shows some regularity, suggesting better control of processing parameters in certain aspects. The distinct areas of varying heights on the surface are clearly identifiable, which aids in further analysis and optimization of processing parameters. Significant height differences between the red and orange regions and the blue and purple regions indicate larger surface unevenness and higher roughness. The non-uniform color distribution reflects a lack of consistency in height variation across the coating surface, which may negatively impact coating performance.

4. Conclusions

(1) The output voltage and deposition frequency are closely related to the surface roughness of the coating. High or low output voltage and deposition frequency will increase the surface roughness of the coating. Therefore, the appropriate voltage and deposition frequency should be selected to ensure the surface quality of the coating.

(2) For electrode speed, excessively high speed does not allow enough time for the coating to distribute on the surface evenly, leading to uneven deposition. Conversely, excessively low speed may increase deposition time and complicate operation, affecting compactness and surface quality.

(3) The optimal process parameters for WC coating deposition on the surface of TC4 titanium alloy were obtained by orthogonal design experiment, which is an output voltage of 120 V, a deposition frequency of 120 Hz, and an electrode speed of 350 r. The coating deposited on the surface of TC4 titanium alloy with the optimal process parameters is the most compact and uniform.

REFERENCES

[1] X.D. Li, Z. Cheng, B.H. Zou, M. Wang, Research status and development trend of electro-spark deposition technology. Electromachining & Mould. **S1**, 18-25 (2024).

[2] H.Y. Zhang, J. Zhang, L. Zhu, T. Wang, Effects of WC content on microstructure and properties of TC4 composite prepared by laser cladding. Hot Working Technology. **51** (8), 83-87 (2022).

[3] H.D. Liu, Y.F. Hu, J.T. Dai, A.Y. Cui, F. Huang, H.B. Li, Effect of ultrasonic vibration on microstructure and hardness of TC4 titanium alloy laser welding joints. Rare Metal Mater. Eng. **47** (2), 624-629 (2018).

[4] J. Zhang, C. Zhu, Progress in research and application of electrospark deposition technology. Materials Reports **37** (21), 221-234 (2023).

[5] H. Xin, H.T. Wang, L. Gao, X. Wang, Y.F. Tan, Research status and development of electro-spark deposition technology. Hot Working Technology **47** (20), 25-29 (2018).

[6] B.Y. Han, X.H. Gao, W.B. Du, W.N. Lei, S.S. Li, M.Q. Cong, W.X. Hang, W. Du, S. Zhu, Technological advances in strengthening the surface wear resistance of aluminum alloys substrate. Materials Reports **37** (10), 157-164 (2023).

[7] Y. Sun, Y. Gao, H. Cheng, Effect of La_2O_3 on microstructure and wear properties of Fe-based coating by electro-spark deposition. Materials Protection **55** (3), 93-97+114 (2022).

[8] A. Equbal, S. Ahmad, I.A. Badruddin, Z.A. Khan, S. Kamangar, J. Syed, Evaluating machining performance of acrylonitrile-butadiene-styrene (ABS) based electrical discharge machining (EDM) electrodes fabricated by fused deposition modelling

(FDM) followed by a novel metallization method. P. I. Mech. Eng. B-J. Eng. **238** (1-2), 164-174 (2024).

[9] P. Zhong, S.S. Si, Z.J. Song, X. Sun, Z.Q. Shi, Y.F. Wang, Effects of processing parameters on surface qualities of electro-spark deposition amorphous coatings,. Hot Working Technology **47** (18), 125-128 (2018).

[10] Y.C. Zhao, Z.Y. Liu, L.L. Yang, Effects of different arc rates on interface behavior of Ni201 repaired layers by electro-spark deppsition. China Mechanical Engineering **27** (10), 1399-1403 (2016).

[11] S. Wang, H.B. Han, S.K. Li, M.N. Li, Analysis of the influence of cylindrical electrode parameters on electro-spark deposition quality based on orthogonal experiment. Transactions of the China Welding Institution **42** (7), 37-43 (2021).

[12] Y. Liu, T.S. Wang, Q.N. Su, F.J. Ma, D.P. Yang, S.F. Zhang, Experimental study on NiCr–3 coating on titanium alloy surface by electro-spark deposition (ESD). Aeronautical Manufacturing Technology **65** (05), 104-112 (2022).

[13] Y. Liu, G.L. Liu, Q.N. Su, J.W. Qu, Z.G. Wang, S.F. Wang, Study on the process law of electro-spark deposition of NiCr-3 coating on titanium alloy. Electromachining & Mould. (6), 26-30 (2021).

[14] G. Kostadinov, T. Penyashki, A. Nikolov, A. Vencl, Improving the surface quality and tribological characteristics of 3D-printed titanium parts through reactive electro-spark deposition. Materials **17** (2), 382 (2024).

[15] W.Q. Wang, M. Du, X.G. Zhang, M.Z. Geng, Microstructure and tribological properties of WC-Ni matrix cermet coatings prepared by electrospark deposition on H13 steel substrate. Acta Metallurgica Sinica **57** (8), 1048-1056 (2021).

[16] Q.S. Huang, Z.G. Chen, X. Wei, L. Wang, Z.W. Hou, W. Yang, Effects of pulse energy on microstructure and properties of Mo_2FeB_2 -based ceramet coatings prepared by electro-spark deposition. China Surface Engineering **30** (3), 89-96 (2017).

[17] J.C. Chen, Influence of Ultrasonic Vibration on the Discharge Mechanism and Surface Quality of Electric Spark Deposition. Henan University of Science and Technology, (2020).

[18] S. Wang, J.Z. Tong, H.B. Han, An automatic control device of contact force for electro-spark deposition and deposition test. Transactions of the China Welding Institution **42** (3), 42-47 (2021).

[19] S. Frangini, A. Masci, A study on the effect of a dynamic contact force control for improving electrospark coating properties. Surf. Coat. Tech. **204** (16/17), 2613-2623 (2010).